Article

Preparation of Nanocomposites of Metals, Metal Oxides, and Carbon Nanotubes via Self-Assembly

Jing Li, Songbai Tang, Li Lu, and Hua Chun Zeng

J. Am. Chem. Soc., **2007**, 129 (30), 9401-9409• DOI: 10.1021/ja071122v • Publication Date (Web): 06 July 2007

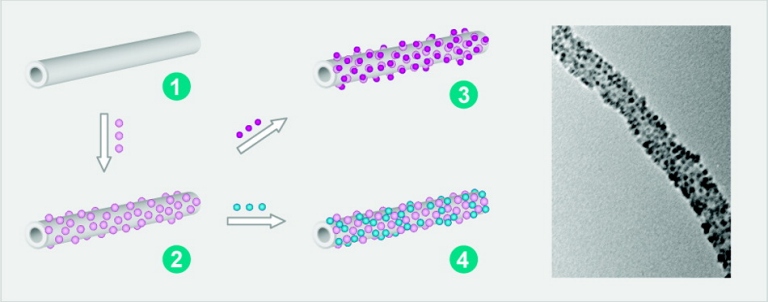

More About This Article

Additional resources and features associated with this article are available within the HTML version:

- Supporting Information
- Links to the 10 articles that cite this article, as of the time of this article download
- Access to high resolution figures
- Links to articles and content related to this article
- Copyright permission to reproduce figures and/or text from this article

View the Full Text HTML

J|A|C|S
ARTICLES
Published on Web 07/06/2007

Preparation of Nanocomposites of Metals, Metal Oxides, and Carbon Nanotubes via Self-Assembly

Jing Li,[†] Songbai Tang,[‡] Li Lu,[‡] and Hua Chun Zeng*,[†]

Contribution from the Department of Chemical and Biomolecular Engineering, Faculty of Engineering, and Department of Mechanical and Production Engineering, Faculty of Engineering, National University of Singapore, 10 Kent Ridge Crescent, Singapore 119260

Received February 15, 2007; E-mail: chezhc@nus.edu.sg

Abstract: Carbon nanotubes (CNTs)-based composites have attracted significant research interest in recent years, owing to their important applications in various technological fields. In this investigation, we describe a general approach to make CNTs-based nanocomposites via self-assembly. The method allows one to prepare binary composites as well as complex systems such as ternary or even quaternary composites where nanoparticles of active phases (e.g., metals and metal oxides) are used as primary building blocks. Six different kinds of binary, ternary, and quaternary nanocomposites, TiO_2/CNTs, Co_3O_4/CNTs, Au/CNTs, Au/TiO_2/CNTs, TiO_2/Co_3O_4/CNTs, and Co/CoO/Co_3O_4/CNTs, have been reported herein in order to draw common features for various assembly schemes. To understand the interconnectivity between the active phases and CNTs, we have devised a range of experiments and examined the resultant samples with many instrumental techniques. On the basis of this work, we demonstrate that highly complex inorganic−organic nanohybrids with good controls in particle shape, size, and distribution can be fabricated from presynthesized nanobuilding units. Concerning their workability, we further show that self-assembled TiO_2/CNTs are sufficiently robust and the electrochemical performance of TiO_2 is significantly enhanced when it is used as a cathode material in Li-battery application.

Introduction

As an emerging class of materials, carbon nanotubes (CNTs)-based nanocomposites have attracted significant research attention in recent years owing to their potential applications in catalysis, chemical sensors, hydrogen storage, and power storage, etc.[1−4] These nanocomposites are commonly prepared by adding a secondary phase (i.e., functional components) to the external surfaces of either single-walled or multiwalled CNTs.[1−4] Structurally, the resultant composites have a phasic (or compositional) variation across the radial direction and a constant concentric arrangement of each participating component along the axial direction, resembling an electric cable configuration.[1−4] There have been numerous ways of fabricating this type of nanocomposites. For example, the conventional impregnation method, sol−gel technique, chemical vapor deposition, electrochemical reduction, and solution growth, including microemulsion technique, have been employed into the preparation, especially for introducing active inorganic components such as noble metals, transition metals, and their oxides and sulfides, Au, Ag, Pt, Rh, Pd, TiO_2, SiO_2, Co_3O_4, Fe_2O_3, ZnO, ZnS, and CdS.[5−27] To enhance interfacial adhesion between an added component and CNTs, surface treatments such as ultrasonication and acid-assisted oxidation have been applied from which new

[†] Department of Chemical and Biomolecular Engineering.
[‡] Department of Mechanical and Production Engineering.

(1) Iijima, S. *Nature* **1991**, *354*, 56−58.
(2) Wildgoose, G. G.; Banks, C. E.; Compton, R. G. *Small* **2006**, *2*, 182−193.
(3) Harris, P. J. F. *Int. Mater. Rev.* **2004**, *49*, 31−43.
(4) H. C. Zeng In *Handbook of Organic−Inorganic Hybrid Materials and Nanocomposites*; American Scientific Publishers: Stevenson Ranch, CA, 2003; Vol. 2: Nanocomposites, Chapter 4, pp 151−180.
(5) Xue, B.; Chen, P.; Hong, Q.; Lin, J.; Tan, K. L. *J. Mater. Chem.* **2001**, *11*, 2378−2381.
(6) Han, L.; Wu, W.; Kirk, F. L.; Luo, J.; Maye, M. M.; Kariuki, N. N.; Lin, Y.; Wang, C.; Zhong, C. J. *Langmuir* **2004**, *20*, 6019−6025.
(7) Correa-Duarte, M. A.; Pérez-Juste, J.; Sánchez-Iglesias, A.; Giersig, M.; Liz-Marzán, L. M. *Angew. Chem., Int. Ed.* **2005**, *44*, 4375−4378.
(8) Aminur Rahman, G. M.; Guldi, D. M.; Zambon, E.; Pasquato, L.; Tagmatarchis, N.; Prato, M. *Small* **2005**, *1*, 527−530.
(9) Qu, J.; Shen, Y.; Qu, X.; Dong, S. *Chem. Commun.* **2004**, 34−35.
(10) Kim, D. S.; Lee, T.; Geckeler, K. E. *Angew. Chem., Int. Ed.* **2006**, *45*, 104−107.
(11) Kim, Y. T.; Ohshima, K.; Higashimine, K.; Uruga, T.; Takata, M.; Suematsu, H.; Mitani, T. *Angew. Chem., Int. Ed.* **2006**, *45*, 407−411.
(12) Sun, C. L.; Chen, L. C.; Sun, M. C.; Hong, L. S.; Chyan, O.; Hsu, C. Y.; Chen, K. H.; Chang, T. F.; Chang, L. *Chem. Mater.* **2005**, *17*, 3749−3753.
(13) Xing, Y. *J. Phys. Chem. B* **2004**, *108*, 19255−19259.
(14) Yoon, B.; Wai, C. M. *J. Am. Chem. Soc.* **2005**, *127*, 17174−17175.
(15) Lu, Y.; Li, J.; Han, J.; Ng, H. T.; Binder, C.; Partridge, C.; Meyyappan, M. *Chem. Phys. Lett.* **2004**, *391*, 344−348.
(16) Kim, H. S.; Lee, H.; Han, K. S.; Kim, J. H.; Song, M. S.; Park, M. S.; Lee, J. Y.; Kang, J. K. *J. Phys. Chem. B* **2005**, *109*, 8983−8986.
(17) Sun, J.; Gao, L.; Iwasa, M. *Chem. Commun.* **2004**, 832−833.
(18) Gomathi, A.; Vivekchand, S. R. C.; Govindaraj, A.; Rao, C. N. R. *Adv. Mater.* **2005**, *17*, 2757−2761.
(19) Banerjee, S.; Wong, S. S. *Nano Lett.* **2002**, *2*, 195−200.
(20) Eder, D.; Kinloch, I. A.; Windle, A. H. *Chem. Commun.* **2006**, 1448−1450.
(21) Pender, M. J.; Sowards, L. A.; Hartgerink, J. D.; Stone, M. O.; Naik, R. R. *Nano Lett.* **2006**, *6*, 40−44.
(22) Fu, L.; Liu, Z.; Liu, Y.; Han, B.; Hu, P.; Cao, L.; Zhu, D. *Adv. Mater.* **2005**, *17*, 217−221.
(23) Sun, Z.; Yuan, H.; Liu, Z.; Han, B.; Zhang, X. *Adv. Mater.* **2005**, *17*, 2993−2997.
(24) Zhu, Y.; Elim, H. I.; Foo, Y. L.; Yu, T.; Liu, Y.; Ji, W.; Lee, J. Y.; Shen, Z.; Wee, A. T. S.; Thong, J. T. L.; Sow, C. H. *Adv. Mater.* **2006**, *18*, 587−592.
(25) Du, J.; Fu, L.; Liu, Z.; Han, B.; Li, Z.; Liu, Y.; Sun, Z.; Zhu, D. *J. Phys. Chem. B* **2005**, *109*, 12772−12776.

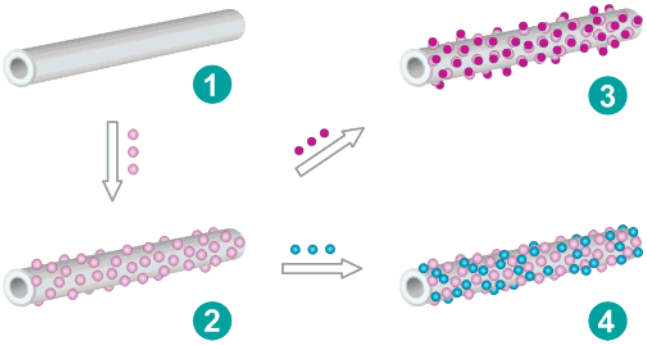

Figure 1. Schematic illustration of the self-assembly schemes for preparation of nanocomposites: (1) carbon nanotubes (CNTs, primary support), (2) a second phase of nanoparticles (in pink) are anchored onto CNTs, (3) a third phase of nanoparticles (in purple) are attached to the surface of the second phase nanoparticles, and (4) a third phase of nanoparticles (in blue) are also landed onto the CNTs. Further addition of phases can also be carried out with the same assembling strategy.

surface functional groups, or additional covalent and/or noncovalent interconnectivity to the secondary phases, may be generated.[28]

Regarding the preparation of the above inorganic−organic hybrid nanocomposites, two basic methods can be further divided. The first one, such as impregnation and sol−gel processes,[5,11,16−18,20,23] requires additional thermal treatments, through which a secondary phase can be formed on the surfaces of CNTs. Owing to the thermal processes, nonetheless, size control and distribution of the surface component become a major difficulty to circumvent if uniform nanocomposites are desired. The second one, such as vapor deposition and solution growth,[2,9,12,22,24−26] depends on a good separation of nucleation and growth steps on the surfaces of CNTs. Because of complex interfacial reactions involved and more demanding process conditions imposed, the same technical challenge in particulate monodispersivity and nucleation site distribution persists in the second method. To explore general techniques for this class of nanocomposites, presynthesized nanoparticles of active components (largely of noble metals) have been loaded directly onto CNTs in recent years. This newer method takes advantage of rapid development of nanomaterials synthesis, as monodisperse inorganic nanoparticles can be prepared routinely nowadays into various colloidal forms. By treating both nanoparticles and CNTs as primary building blocks, several binary nanocomposites have been fabricated with the self-assembly approach very recently.[6−8,19,27]

Apart from the binary nanocomposites, from a fundamental viewpoint, it would be highly desirable to develop some general methodologies to make CNTs-based nanocomposites via self-assembly, which will allow us to prepare binary composites as well as complex systems such as ternary or even quaternary composites using the same architectural concepts. In this article, as summarized in Figure 1, we will present a systematic investigation on self-assemblies of presynthesized metal/metal oxide nanobuilding blocks on CNTs. In particular, six material combinations, TiO_2/CNTs, Co_3O_4/CNTs, Au/CNTs, Au/TiO_2/CNTs, TiO_2/Co_3O_4/CNTs, and Co/CoO/Co_3O_4/CNTs, have been prepared in this work in order to draw common features of the various assembly schemes (Figure 1). The interconnectivity between the overlayers and CNTs has also been studied with different analytical techniques. Our investigation shows that self-assembly indeed can be a general approach to make highly complex inorganic−organic nanohybrids with good controls in particle shape, size, concentration, and distribution. Using the prepared TiO_2/CNTs nanocomposite as a model system, furthermore, we demonstrate that the assembled material is sufficiently robust and its electrochemical performance is significantly improved when used as a cathode material in Li-battery application.

Experimental Section

Synthesis of TiO_2 Suspension. The suspension of monodisperse TiO_2 nanoparticles was prepared according to a reported process with some modifications.[29] Briefly, 0.1 mL of *tert*-butylamine was added to 10.0 mL of deionized water. At the same time, 0.11 g of Ti−*n*-propoxide (98%, Alfa Aesar) and 6.0 mL of oleic acid (OA, $CH_3(CH_2)_7$-$CH{=}CH(CH_2)_7COOH$, 90−95%, Alfa Aesar) were added to 10.0 mL of toluene. The above two solutions were then mixed and transferred to a Teflon-lined stainless steel autoclave. Hydrothermal synthesis was conducted at 180 °C for 6 h in an electric oven. After the reaction, the organic phase (toluene) was separated from the aqueous phase and added with 10 mL of methanol as a flocculant in order to sedimentate TiO_2 product. Followed by two cycles of centrifugation and decantation, OA-capped TiO_2 nanoparticles were redispersed into 4 mL of toluene in a glass sample vial ready for use. This suspension showed a clear light yellow color which was stable for a storage time of more than 2 months at room temperature.

Preparation of TiO_2 Powder. In order to obtain the TiO_2 powder for XPS study, much more methanol was used to remove the OA capping on TiO_2 nanoparticles in the above TiO_2 suspension. In detail, 25 mL of methanol was used each time and a total of five times of centrifugation and decantation was applied. After that, the white sample was dried at 60 °C overnight for XPS analysis. The OA capping had been partially removed from TiO_2 nanoparticles because this product could not be redispersed into toluene, i.e., agglomeration of TiO_2 nanoparticles had taken place when the TiO_2 powder was prepared.

Synthesis of Co_3O_4 Nanoparticles. Freestanding discrete Co_3O_4 nanoparticles (dried powder, in a cubic form) were obtained by refluxing a $Co(NO_3)_2$ precursor solution at 95 °C for 72 h with Tween-85 as a surfactant, as had been detailed in our previous investigation.[30] The Co_3O_4 nanoparticles were precipitated by adding ethanol as a flocculant and washed with copious ethanol for several times. Unlike the above TiO_2 powder, dried Co_3O_4 nanocubes did not coalesce together and they could be redispersed easily in ethanol solvent again.

Oxidation of CNTs in Nitric Acid. An amount of 50 mg of as-received multiwalled CNTs (from Aldrich) were treated in 100 mL of 6 M nitric acid (HNO_3) for 3−15 h under ultrasonic conditions (in an ultrasonic water bath; Elma, Elmasonic S10, 30 W, 50/60 Hz).

Preparation of TiO_2/CNTs Nanocomposites. An amount of 0.01−0.11 g of the as-received CNTs or HNO_3-treated CNTs was first dispersed in 4−60 mL of toluene in the above-mentioned ultrasonic water bath for 0.5−2 h. Afterward, 1−8 mL of the TiO_2 suspension (in toluene) was added, and the mixture was continuously sonicated for another 0.5−1 h. The same TiO_2/CNTs nanocomposites were also assembled under mechanical stirring condition for a longer process time of 12 h without assistance of sonication. The resultant TiO_2/CNTs product was washed thoroughly with toluene and ethanol solvents and dried in an electric oven at 60 °C for several hours.

Preparation of Co_3O_4/CNTs Nanocomposites. An amount of 0.5−10.0 mg of CNTs (as received from Aldrich without any acid treatment)

(26) Liu, B.; Lee, J. Y. *J. Phys. Chem. B.* **2005**, *109*, 23783−23786.
(27) Robel, I.; Bunker, B. A.; Kamat, P. V. *Adv. Mater.* **2005**, *17*, 2458−2463.
(28) Xing, Y.; Li, L.; Chusuei, C. C.; Hull, R. V. *Langmuir* **2005**, *21*, 4185−4190.
(29) Pan, D.; Zhao, N.; Wang, Q.; Jiang, S.; Ji, X.; An, L. *Adv. Mater.* **2005**, *17*, 1991−1995.
(30) Xu, R.; Zeng, H. C. *Langmuir* **2004**, *20*, 9780−9790.

was added with 2−20 mL of ethanol and 0−20 mL of 0.1 M maleic acid (*cis*-butenedioic acid ($HO_2CCH{=}CHCO_2H$), dissolved in ethanol). After sonicating the above mixture for 15 min, 5−100 mg of Co_3O_4 powder was added, and the mixture was continuously stirred overnight in most cases. Short assembling times of 20 min to 4 h were also adopted in this study. Before drying, the as-prepared Co_3O_4/CNTs product was washed with ethanol for three times.

Preparation of Au/CNTs Nanocomposites. The Au nanoparticle suspension used herein was prepared according to a two-phase protocol reported in the literature.[31] Briefly, 0.19 g of tetraoctyl-ammonium bromide (TOAB) was first dissolved in 7.0 mL of toluene, which was then mixed with 4 mL of 0.01 M chloroauric acid ($HAuCl_4$) aqueous solution with vigorous stirring. Afterward, 1.0 mL of 0.22 M 1-dodecanethiol ($C_{12}H_{25}SH$, in toluene) was added. Under the same stirring condition, 3.0 mL of 0.1 M $NaBH_4$ was added to commence chemical reactions.[32] About 1.0 mL of 0.22 M 3-mercaptopropionic acid (MPA, $HS(CH_2)_2COOH$ in toluene; as a molecular linker) was added to 5 mg of HNO_3-treated CNTs (15 h), followed by adding 0.5 mL of the Au nanoparticle suspension. The system was sonicated in the ultrasonic water bath for 10 min and kept still for another 3 h. The prepared Au/CNTs samples were washed with acetone for three times prior drying.

Preparation of Au/TiO_2/CNTs Nanocomposites. (i) Photoassisted method: About 5.0 mg of TiO_2/CNTs powder was added with 0.04 mL of 0.01 M $HAuCl_4$ (pH 7, using a 1.0 M NaOH solution to adjust) and 4 mL of deionized water. After the aforementioned ultrasonic treatment for 5 min, it was irradiated with a UV mercury high-pressure vapor lamp (light intensity at 365.5 nm = 213 W/m^2; HPR 125 W) for 4 min. The product was washed with deionized water for several times. In other experiments, 1.0 mL of 0.05 wt % polyvinylpyrrolidone (PVP) was also added to the above precursor system to control the morphology of Au nanocrystals. This mixture was sonicated for 10 min and then irradiated under the same UV light for 5−30 min. The products received the same treatments afterward. (ii) Molecular linker method: To prepare self-assembled Au/TiO_2/CNTs, about 5 mg of TiO_2/CNTs powder was dispersed to 0.5 mL of 0.44 M MPA (in toluene; as a molecular linker) with the same ultrasonic treatment. After that, 0.5 mL of the as-prepared Au nanoparticle suspension (in toluene; refer to the preparation of Au/CNTs above) was added under the sonicating condition. The resultant Au/TiO_2/CNTs was washed with toluene and ethanol for several times.

Preparation of TiO_2/Co_3O_4/CNTs Nanocomposites. About 5 mg of the Co_3O_4/CNTs dried powder was redispersed in 3 mL of toluene using the above ultrasonic treatment. A volume of 1 mL of this suspension was added with 0.2 mL of the as-prepared TiO_2 suspension (in toluene), and the mixture was sonicated for another 30 min. Finally, the sample was washed with toluene and ethanol, respectively, for several times.

Preparation of Unsupported TiO_2/Co_3O_4 Nanocomposites. Large Co_3O_4 nanocubes with edge length of 30−50 nm were prepared according to an earlier report.[33] In the present work, 10 mg of the prepared Co_3O_4 nanocubes were dispersed to 1 mL of toluene under the same ultrasonic conditions. To this mixture, 2 mL of maleic acid solution (0.1 M, in ethanol) and 2 drops of the TiO_2 nanoparticle suspension (in toluene) were added. The product composite was sonicated for another 30 min and washed with toluene for three times.

Preparation of Co/CoO/Co_3O_4/CNTs Nanocomposites. About 50 mg of Co_3O_4/CNTs sample was purged with Ar gas inside a quartz tube reactor at a flow rate of 70 mL/min to 500 °C (the heating rate was 10 °C/min). A stream of pure hydrogen was then introduced at a rate of 50 mL/min, and the sample was held at 500 °C for 2 h. The composite samples (Co/CoO/Co_3O_4/CNTs) were collected when the furnace temperature was decreased to room temperature.

Materials Characterization. The crystallographic information of the as-prepared samples was investigated using powder X-ray diffraction (XRD, Shimadzu X-ray diffractometer, model 6000, Cu Kα radiation $\lambda = 1.5406$ Å) at a scanning rate of 2° min^{-1}. Field emission scanning electron microscopy (FESEM, JSM-6700F) was employed to examine the morphologies of the nanocomposites prepared. Structural and compositional investigation with transmission electron microscopy and X-ray energy dispersive spectroscopy (TEM and HRTEM) was carried out on a JEM-2010 and a JEM-2010F with an electron kinetic energy of 200 kV.[34] Compositional investigation for the samples was carried out with X-ray photoelectron spectroscopy (XPS; AXIS-HSi, Kratos Analytical) and energy dispersive X-ray spectroscopy (EDX, JEM-2010/EDX).[35] The content of CNTs in the nanocomposite samples was determined using a thermogravimetric method (TGA, TA instrument TGA 2050). About 10 mg of the dried samples was heated with an air flow of 100 mL·min^{-1} and at a heating rate of 10 °C·min^{-1} from room temperature to 800 °C.

Results and Discussion

Experimental details on all reported samples in this work can be found in Supporting Information (SI-1). Figure 2 shows some representative microscopic images of the TiO_2/CNTs nanocomposites and their starting building blocks. The as-prepared anatase TiO_2 nanoparticles used in this material system have a narrow size distribution of 3−4 nm. In comparison to the as-received sample (Figure 2b), the CNTs surface becomes rougher and coarser after loaded with TiO_2 nanoparticles, as shown in the panoramic views of these samples (e.g., Figure 2c). With the present method, the metal oxide nanoparticles can be dispersed evenly. Detailed distributions of TiO_2 and Co_3O_4 nanoparticles on CNTs are examined in Figures 2−4. Due to their monodisperse cubic shape (4−5 nm in size) and more bulky capping molecules for hydrophobic interactions, in particular, the Co_3O_4 nanoparticles seem to exhibit more ordered alignment than the TiO_2 nanoparticles which are less faceted. At a low surface content, as detailed in Figure 3a, a monolayer or submonolayer of discrete oxide nanoparticles can be assembled. This observation suggests that the attractive interaction between the nanoparticles and CNTs support is stronger than the van der Waals interactions among the headgroups of organic capping of the metal oxides. An XPS investigation on this aspect will be presented in a later part of this work.

XRD investigations for the above two composite systems are reported in Figure 5. Although the (101) diffraction of the metal oxide phase overlaps a little with the (002) of CNTs, it is affirmed that the TiO_2 nanoparticles still maintain their pristine phase after connecting to the CNTs; all diffraction peaks can be indexed to tetragonal anatase TiO_2 (space group: $I4_1/amd$; $a_0 = 3.79$ Å and $c_0 = 9.51$ Å; JCPDS file no. 21-1272).[36] Similarly, the XRD pattern of Co_3O_4/CNTs nanocomposite shows three strong peaks of spinel phase, confirming that the Co_3O_4 is still in its original structure (space group: $Fd3m$, lattice constant $a_0 = 0.81$ nm; JCPDS file no. 43-1003).[37−39] Diffraction peaks from the CNTs support cannot be detected in this latter case, because of a small quantity of CNTs used in this case and an overwhelming diffraction signal from the Co_3O_4 phase.

(31) Brust, M.; Walker, M.; Bethell, D.; Schiffrin, D. J.; Whyman, R. *J. Chem. Soc., Chem. Commun.* **1994**, 801−802.
(32) Li, J.; Zeng, H. C. *Chem. Mater.* **2006**, *18*, 4270−4277.
(33) (a) Feng, J.; Zeng, H. C. *Chem. Mater.* **2003**, *15*, 2829−2835. (b) Chen, H. M.; Liu, R.-S.; Li, H. L.; Zeng, H. C. *Angew. Chem., Int. Ed.* **2006**, *45*, 2713−2717.
(34) Liu, B.; Zeng, H. C. *J. Am. Chem. Soc.* **2004**, *126*, 16744−16746.
(35) Li, J.; Zeng, H. C. *Angew. Chem., Int. Ed.* **2005**, *44*, 4342−4345.
(36) Yang, H. G.; Zeng, H. C. *J. Phys. Chem. B* **2003**, *107*, 12244−12255.
(37) Sugimoto, T.; Matijević, E. *J. Inorg. Nucl. Chem.* **1979**, *41*, 165−172.
(38) Matijević, E. *Chem. Mater.* **1993**, *5*, 412−426.
(39) Ocana, M.; Gonzalez-Elipe, A. R. *Colloids Surf., A* **1999**, *157*, 315−324.

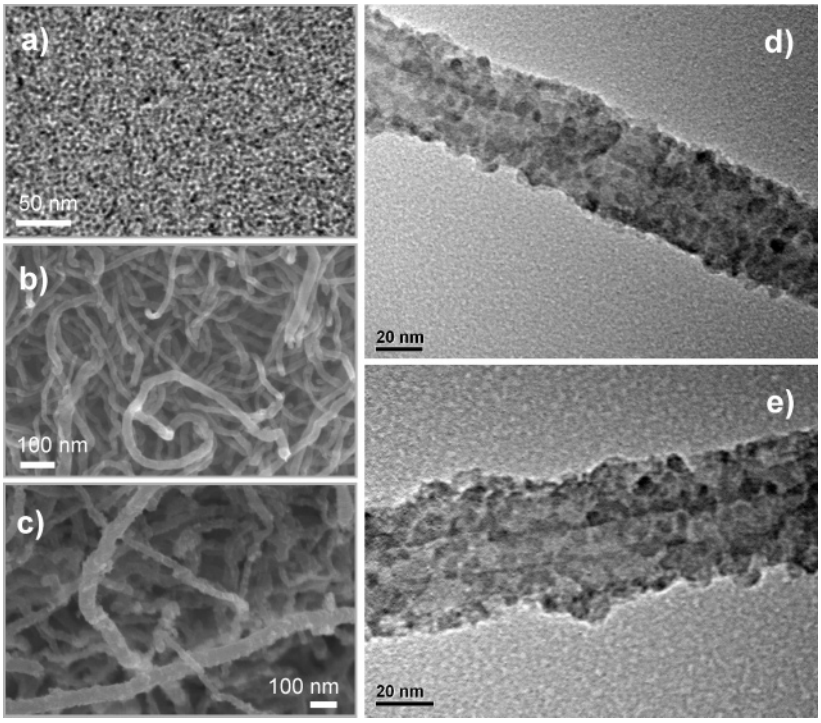

Figure 2. (a) As-synthesized TiO_2 nanoparticles (TEM image), (b) raw CNTs (FESEM image), (c) as-prepared TiO_2/CNTs nanocomposite (FESEM image), and (d and e) detailed views on the TiO_2/CNTs nanocomposite (TEM images).

The sonochemical oxidation of CNTs to generate surface functional groups in strong acidic solutions (e.g., H_2SO_4 and HNO_3) has been recently investigated.[13,28] It has been shown that surface roughness and thus surface functional groups (such as carboxylate anions, etc.) are increased with this sonochemical treatment, whereas no measurable changes in diameters and lengths can be found.[13,28] In our present work, however, we found no major difference in the products when the as-received (raw) or the acid-treated CNTs (Supporting Information SI-2) was used. This finding indicates that our raw CNTs have contained sufficient active sites and functional groups for self-assembly of inorganic phases. For this reason, unless otherwise specified, only the as-received CNTs were used in this work (see the Experimental Section). Nonetheless, the ultrasonic process we adopted might cause certain alternation of wall structures to the as-received CNTs.[13,28] In Figure 3, for instance, although the oxide particles are highly crystalline the graphene layers of sonicated CNTs apparently become less continuous in the product nanocomposite; this observation also accounts for the weak (or undetectable) intensity of the CNTs phase in our XRD patterns (Figure 5). The attained self-assemblies can be attributed to at least three types of interactions. First, ionic interactions between the metal oxide and CNTs may play a significant role. For instance, carboxylate groups on the CNTs will provide bonding to the TiO_2 and Co_3O_4 nanoparticles,[30,40] as revealed by our XPS investigation that will be discussed shortly. In the case of TiO_2/CNTs, the combination of two assembling phases can be described as a partial replacement of carboxylate ends of OA of TiO_2 nanoparticles with the carboxylate groups of CNTs, that is, the carboxylate anions of CNTs now bind directly to the TiO_2, noting that relatively simple chemical reagents were selected in this assembling process. Although sonication would shorten the assembling time to a range of 0.5−1 h, the same self-assembly could also be carried out under simple mechanical stirring without sonication. This process was also adopted in our preparation of TiO_2/CNTs nanocomposites (Supporting Information SI-3), and it was taken as a major preparative method for Co_3O_4/CNTs system, because sonication could cause some agglomeration of Co_3O_4 nanocubes owing to a stronger hydrophobic interaction among their bulky surfactant capping, i.e., alkylated oleate groups [in the ionic form of $CH_3(CH_2)_7CH{=}CHCH_2CR_2(CH_2)_5COO^-$, where R represents for $CH_2CH{=}CHCH_2$ $(CH_2)_6CH_3$],[30,40] compared to the simple oleate groups of OA on the TiO_2. Under stirring condition, however, the self-assembly of Co_3O_4 onto CNTs tends to be slower. For example, appreciable combination of the Co_3O_4 to CNTs only took place after 2−4 h of stirring. Second, hydrophobic interactions between headgroups of organic capping and graphene layers of CNTs may account for another type of binding capacity in composite construction,[2,6,7,27] noting that there are abundant straight/branched aliphatic hydrocarbon chains on the oxide surfaces to provide this noncovalent linkage, though it may not be as strong. And third, hydrogen bonding among the carboxylic, hydroxyl, and/or ether functional groups in both metal oxide and CNTs phases may also be partially responsible for the observed interconnectivity.[2,6] It should be mentioned that the above integrative forces between the over layer nanoparticles and CNTs are rather effective, as all our samples reported herein had undergone extensive washing and sonication treatments.

To identify key bonding factors, we found that using maleic acid (see the Experimental Section), which has two carboxyl groups in each end of the molecule, did not cause distinguishable changes among the assembled Co_3O_4/CNTs products, as compared in Figure 4. If it is present, maleic acid will interact with existing hydrogen bonding between the oxide and CNTs and lead to either interruption or detachment of the two phases

(40) Yao, K. X.; Zeng, H. C. *J. Phys. Chem. B* **2006**, *110*, 14736−14743.

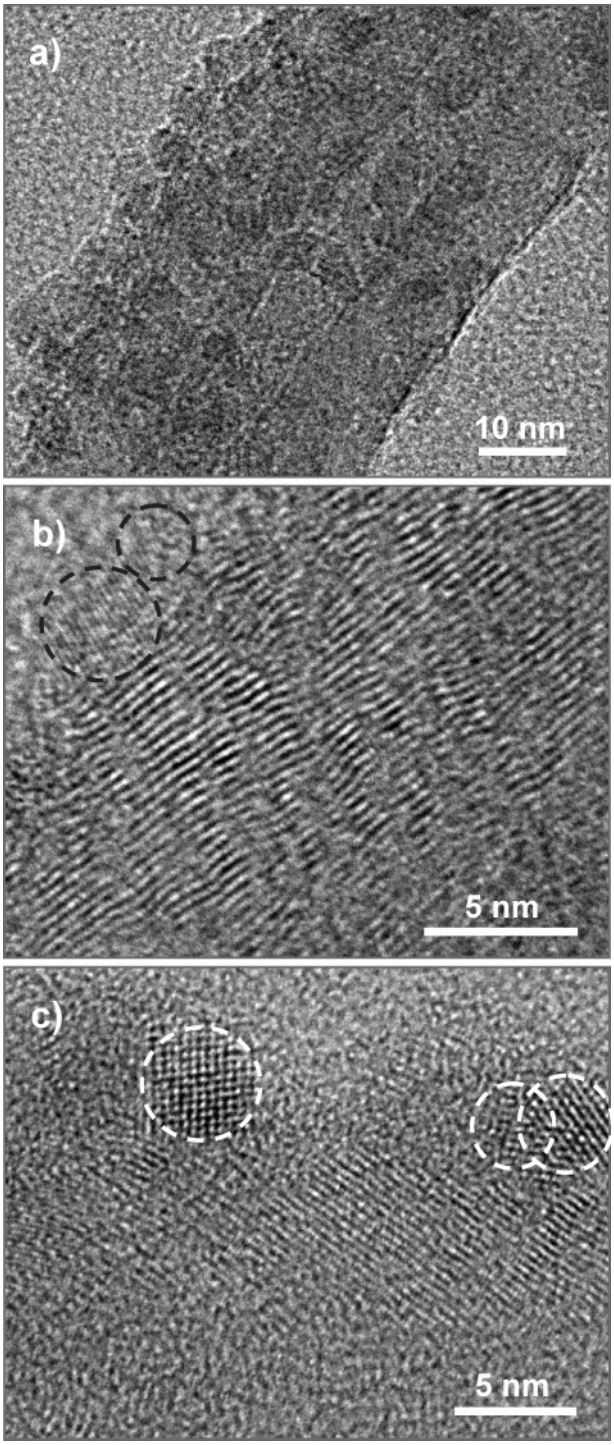

Figure 3. HRTEM images of the as-prepared TiO_2/CNTs nanocomposite: (a) overall structure, (b) defective wall structure, and (c) crystalline TiO_2 nanoparticles on CNTs. Anatase TiO_2 particles are circled in (b) and (c).

considering its richness in carboxyl groups. We now understand that hydrogen bonding may not be a predominant cause for the observed biphasic assemblies. According to our XPS study, which will be discussed in detail shortly, it is suggested that the attachment of the Co_3O_4 to CNTs substrate also depends on a replacement of the alkylated oleate groups of the Co_3O_4 nanocubes with carboxylate groups of the CNTs. The self-assembled Co_3O_4/CNTs nanocomposites are also expected to be stable. To confirm this, we have treated these samples in

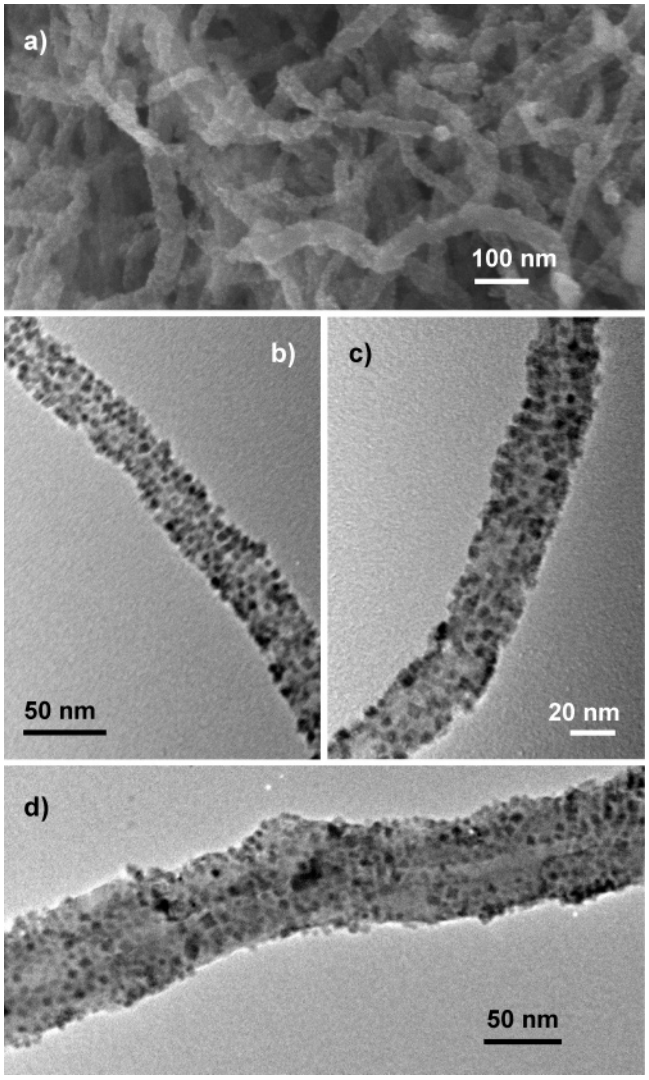

Figure 4. (a) Large view on as-prepared Co_3O_4/CNTs nanocomposite (FESEM image), (b and c) detailed views (TEM images) on as-prepared Co_3O_4/CNTs nanocomposites, and (d) the Co_3O_4/CNTs nanocomposite synthesized without using maleic acid (TEM image).

sonicating environment and found they remained largely intact after the treatment.

On the basis of the above binary nanocomposites, additional components of metal oxides or metals can be further introduced one at a time. In general, three basic methods, self-assembly, crystal growth, and chemical conversion, can be readily employed to add a third or a fourth chemical component to the existing binary basis. In this way, the present approach also allows us to fabricate even more complex ternary or quaternary composites (schemes 3 and 4, Figure 1). To elucidate methodic generality, we have also prepared three different ternary/quaternary nanocomposites, i.e., Au/TiO_2/CNTs, TiO_2/Co_3O_4/CNTs, and Co/CoO/Co_3O_4/CNTs; the related synthetic processes of these composites can be found in the Experimental Section.

Figure 6, parts a and b, shows the Au/TiO_2/CNTs prepared with a photoassisted growth of Au on a premade TiO_2/CNTs (Supporting Information SI-4a). As expected for this conventional process, the grown Au nanoparticles are polydisperse and randomly distributed. With assistance of PVP, nonetheless, shapes of Au nanocrystals can be further controlled for this composite under similar reaction conditions (Supporting Infor-

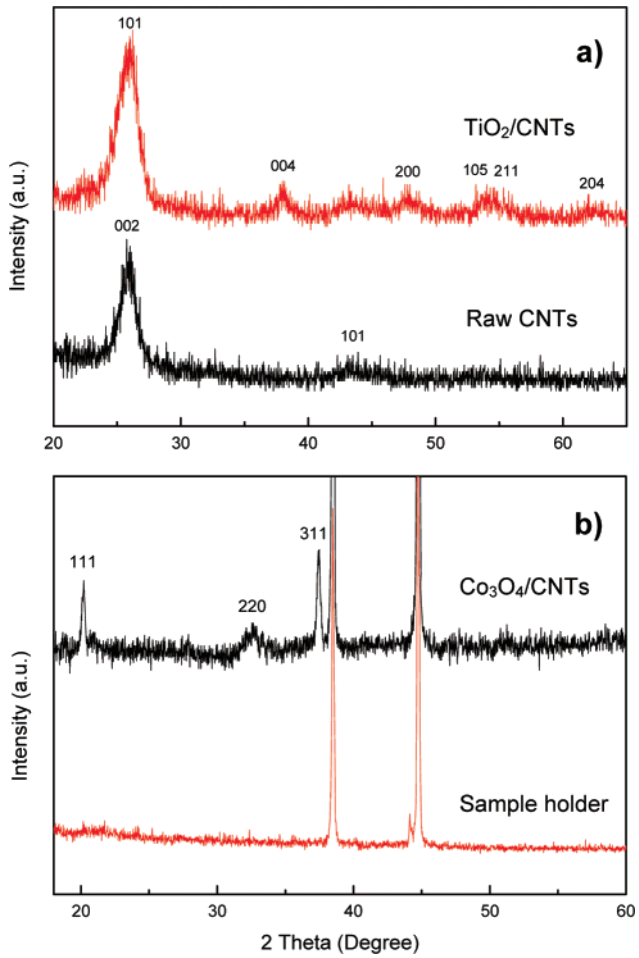

Figure 5. XRD patterns of (a) as-prepared TiO_2/CNTs nanocomposite and as-received CNTs and (b) as-prepared Co_3O_4/CNTs nanocomposite (using an aluminum sample holder).

mation SI-4b), but the particles are quite large. But if we adopt a self-assembly approach, i.e., introduced presynthesized monodisperse Au nanoparticles to the TiO_2 with assistance of MPA linker, much more uniform Au/TiO_2/CNTs can be obtained (Figure 6c and Supporting Information SI-4c). In accordance to scheme 3 of Figure 1, however, the Au nanoparticles in both cases were grown or attached more favorably on the TiO_2 surface than onto the CNTs. In the photoassisted metal growth, for example, an electron−hole pair is first created within TiO_2 upon the UV light irradiation, which provides nucleation sites for reductive deposition of Au nanoparticle, as discussed in our previous investigation.[32] In the latter case, on the other hand, the carboxylate moiety of MPA is expected to chelate onto Lewis sites of the TiO_2 surface,[30,32] rather than to the CNTs. To further verify this scheme of Au attachment, we have also fabricated simple binary composites of Au/CNTs. Our result shows that it is indeed more difficult to add the Au nanoparticles directly onto CNTs (i.e., scheme 4; Supporting Information SI-5). In the preparation of TiO_2/Co_3O_4/CNTs (Figure 6d), we found that TiO_2 nanoparticles can deposit on Co_3O_4 as well as CNTs surfaces (Supporting Information SI-6); the net result thus corresponds to a mixed state of schemes 3 and 4, Figure 1. The additional interconnectivity between TiO_2 and Co_3O_4 nanoparticles, though it may be weaker, can be attributed to a hydrophobic interaction among the surfactant capping molecules. To explore this point further, Figure 7 examines an unsupported TiO_2/Co_3O_4 nanocomposite fabricated from large Co_3O_4 nanocubes and small TiO_2 nanoparticles (see the Experimental Section and Supporting Information SI-7). Since they have two carboxylate groups, maleic acid molecules in this case work as a bidentate linker to bring the two oxide phases together, noting that there is no organic capping in these large as-prepared Co_3O_4 nanocubes. Using the Co_3O_4/CNTs precursors, on the other hand, we have also prepared metal/oxides/CNTs composites, Co/CoO/Co_3O_4/CNTs using a gaseous reduction route (Supporting Information SI-8). It has been found that the CNTs-supported Co_3O_4 nanocubes can be converted to metallic cobalt in the atmosphere of hydrogen. In particular, intermediate oxide phase CoO can also be present in this reductive reaction, giving the quaternary composite system (Supporting Information SI-8).

The content of organic phase CNTs in the prepared nanocomposites can be determined facilely with the TGA technique via oxidative decomposition. Figure 8 shows some representative TGA and DrTGA curves of the TiO_2/CNTs and Co_3O_4/CNTs nanocomposites, together with those of the as-received CNTs for reference (Figure 8a). For the TiO_2/CNTs sample, the first weight loss in a broad temperature range of 220−380 °C is due to the oxidative decomposition of the organic capping (OA) on the TiO_2 nanoparticles surface. The CNTs are decomposed at about 460−680 °C, which shows a small shift to lower temperatures with respect to those of the pristine CNTs; the shift observed can be thus attributed to a weak catalytic effect of the TiO_2 nanoparticles (Figure 8, part b vs part a). For the Co_3O_4/CNTs, the first two peaks at 148 and 204 °C can be both ascribed to the decomposition of organic capping (i.e., alkylated oleate ions). But compared with the TiO_2/CNTs, the CNTs of the Co_3O_4/CNTs decompose in a much lower temperature range of 270−430 °C. This can be attributed to the catalytic role of Co_3O_4 nanoparticles to oxidation of carbon materials.[33] The two examples shown here represent the highest loadings attainable in this work for the two metal oxide phases on the CNTs support, i.e., about ∼43 wt % for TiO_2 and ∼61 wt % for Co_3O_4, respectively. In the same way, other nanocomposites with metal oxide contents (practically starting from ∼0 wt %) lower than the above maxima values can be tailor-made by selecting ratios of assembled components, i.e., oxide/CNTs ratio, etc., and assembling time used. In general, a greater oxide/CNTs ratio and a longer process time will give a higher content of oxide phase in the resultant nanocomposites.

In order to shed light on the chemical nature of interconnection between the oxide phase and CNTs, we also carried out XPS investigations for both TiO_2/CNTs and Co_3O_4/CNTs systems. In Figure 9, spectra of all studied elements were referenced to the C 1s peak (binding energy BE = 284.6 eV) arising from adventitious carbon,[32,35] sp^2-hybridized carbon of the CNTs, and/or the aliphatic hydrocarbon chains of the surfactant OA.[30,41] The other two small peaks of the dried TiO_2 powder are positioned at 286.1 and 288.7 eV, respectively. The peak at 286.1 eV can be assigned to hydroxyl carbon (C−OH),[42] and the peak at 288.7 eV can be assigned to carboxyl carbon (O═C−O).[42] Besides the main peak at 284.6 eV, both TiO_2/CNTs nanocomposites and raw CNTs have a peak at 285.5 eV

(41) Lee, K. Y.; Kim, M.; Hahn, J.; Suh, J. S.; Lee, I.; Kim, K.; Han, S. W. *Langmuir* **2006**, *22*, 1817−1821.
(42) Kovtyukhova, N. I.; Mallouk, T. E.; Pan, L.; Dickey, E. C. *J. Am. Chem. Soc.* **2003**, *125*, 9761−9769.

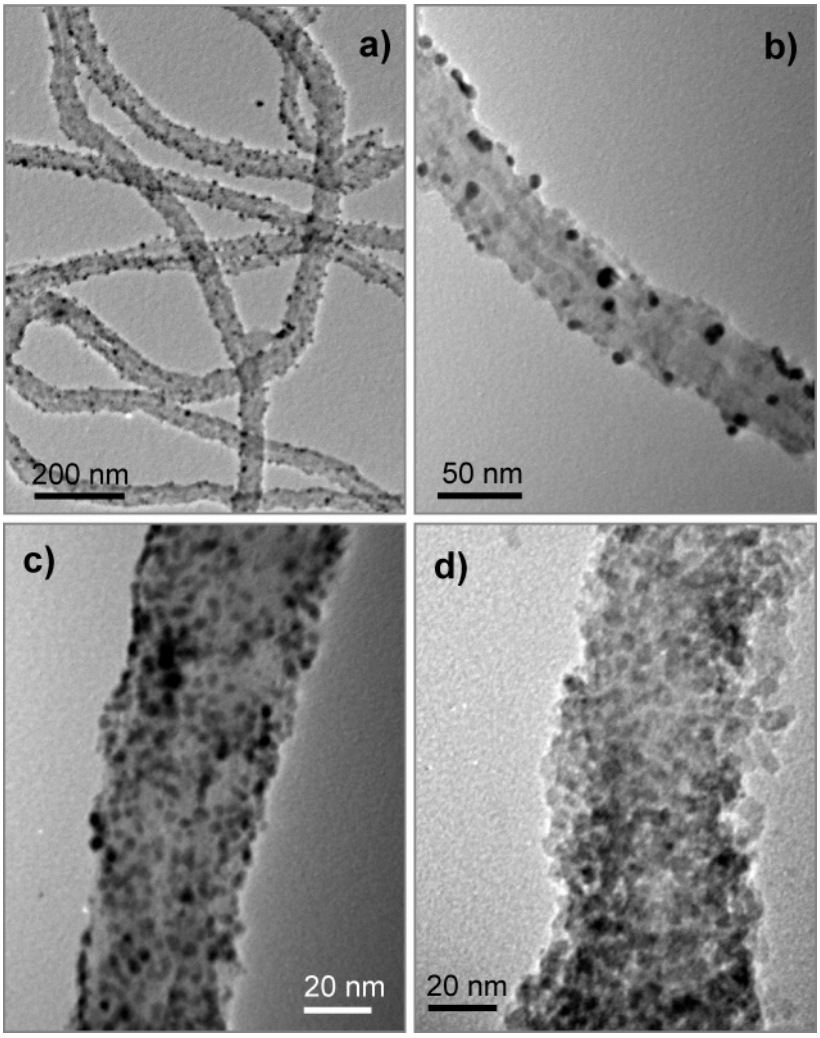

Figure 6. Ternary nanocomposites (TEM images): (a and b) a large view and a detailed view on the Au/TiO_2/CNTs nanocomposites prepared by the photoassisted method, (c) a detailed view on the Au/TiO_2/CNTs prepared by the self-assembly method, and (d) a detailed view on the TiO_2/Co_3O_4/CNTs nanocomposite prepared by the self-assembly method.

which can be attributed to defect-containing sp^2-hybridized carbon.[41] This peak (285.5 eV) becomes more pronounced in the TiO_2/CNTs, as the CNTs in this composite have undergone sonication processes. In comparison to raw CNTs, the additional peak at 286.4 eV is assigned to the oxidized species C−O on the nanotube surface, which is expectable because there are more defective sp^2-hybridized carbons and the CNTs become more prone to oxidation. Consistent with this observation, the defect-containing sp^2-hybridized carbon also increases in the Co_3O_4/CNTs composites when they undergo sonication treatment, on the basis of an XPS analysis for C 1s spectra (Supporting Information SI-9).

The TiO_2 powder after washing and drying shows an irreversible aggregation of the TiO_2 nanoparticles, and this sample gives two characteristic peaks of Ti 2p at 458.5 and 464.1 eV that well correspond to the normal BEs of TiO_2.[36] Because of partial removal of their surface OA molecules during the washing, which caused an aggregative growth, the dried TiO_2 powder could not be redispersed back to a colloidal suspension. In contrast, TiO_2 nanoparticles could prevent this type of particle coalescence, if they were loaded on CNTs directly from their as-prepared suspensions. In this sample, Ti 2p BEs are shifted to 459.5 and 465.1 eV, respectively. The observed BE shifts are primarily due to the difference in oxide particle size, dispersion states, ligand effect, and electronic interaction between the surface oxide and CNTs substrate,[41,43−47] which will be further addressed in their O 1s spectra below. On the other hand, there is no observable shift for the Co 2p peaks in the Co_3O_4/CNTs, compared to the dried Co_3O_4 nanocubes (Supporting Information SI-9). This is because the organic capping on Co_3O_4 nanocubes is more difficult to remove and there is no major change in their nanoparticulate state in either case.

The O 1s spectrum of the dried TiO_2 powder is deconvoluted into four peaks, and they can be assigned to lattice oxygen in anatase TiO_2 (529.8 eV), surface Ti−OH or O−C═O (531.6 eV), C−O−H and/or C−O−C group (532.4 eV), and adsorbed H_2O molecules (533.4 eV), respectively.[32] These carbon−oxygen species indicate the presence of OA molecules on this TiO_2 even after the particulate coalescence. Although they can be attributed to the same oxygen species, the positions of the

(43) Kim, Y. T.; Mitani, T. *J. Catal.* **2006**, *238*, 394−401.
(44) Cheung, T. T. P. *Surf. Sci.* **1984**, *140*, 151−164.
(45) Wertheim, G. K.; DiCenzo, S. B.; Youngquist, S. E. *Phys. Rev. Lett.* **1983**, *51*, 2310−2313.
(46) Eberhardt, W.; Fayet, P.; Cox, D. M.; Fu, Z.; Kaldor, A.; Sherwood, R.; Sondericker, D. *Phys. Rev. Lett.* **1990**, *64*, 780−783.
(47) Mason, M. G. *Phys. Rev. B* **1983**, *27*, 784−762.

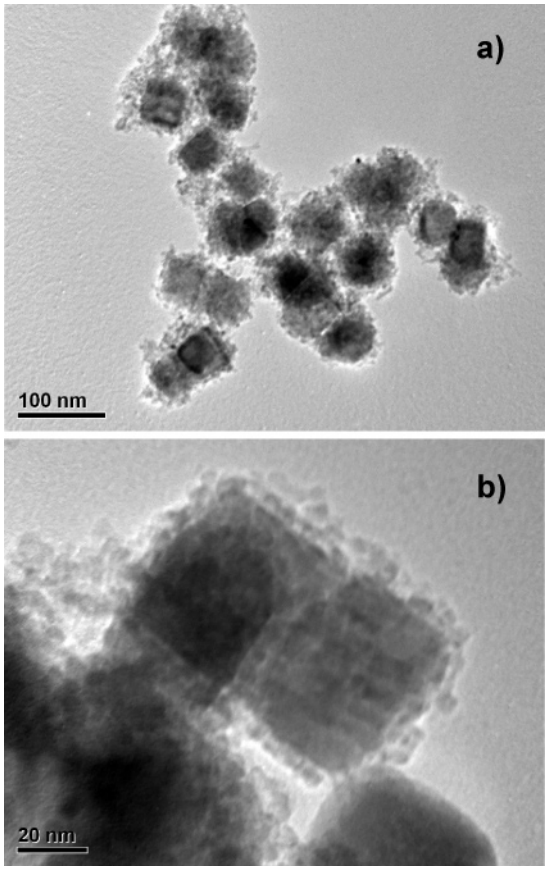

Figure 7. Unsupported TiO_2/Co_3O_4 nanocomposite (TEM images): (a) overall morphology and (b) a detailed view on the surface regions. The TiO_2 nanoparticles on the surface are in the size range of 3−4 nm, while Co_3O_4 nanocubes (edge length at 30−50 nm) act as core templates in this core−shell nanostructure.

O 1s peaks from the TiO_2/CNTs composites are nevertheless different from those of the dried TiO_2 powder. Similar to their Ti 2p spectra, O 1s peaks from the TiO_2/CNTs composites are also shifted toward higher BEs. For example, the lattice oxygen in anatase TiO_2 is now about 0.6 eV higher than that in the dried TiO_2 phase. The positive shifts in BEs are consistent with the similar trend observed in the Ti 2p spectra which has been ascribed to the monodisperse nature of TiO_2 nanoparticles in the TiO_2/CNTs and the stronger electronic interaction (i.e., charge transfer from the surface TiO_2 to CNTs), noting that all the BEs discussed herein are referred to the sp^2-hybridized carbon of CNTs at 284.6 eV and the actual negative BE shifts of CNTs cannot be noted explicitly. In this agreement, similar positive BE shifts are also observed in the TiO_2/CNTs assembled with mechanical stirring (Supporting Information SI-3 and SI-10). On the other hand, the as-received CNTs also have three O 1s peaks positioned at 531.1 (carbonyl, −C═O), 532.4 (carboxyl, C−OH), and 533.6 eV (H_2O molecules), respectively, which are due to a certain degree of oxidization on the pristine CNTs surface.[48,49] It has been found that the O 1s peaks will shift toward higher BEs with ultrasonic treatment in acid. On the basis of our HRTEM observation, we also see that the CNTs become more defective in our ultrasonic dispersion. In this regard, therefore, the O 1s peaks at 531.9−531.1, 532.8−532.4,

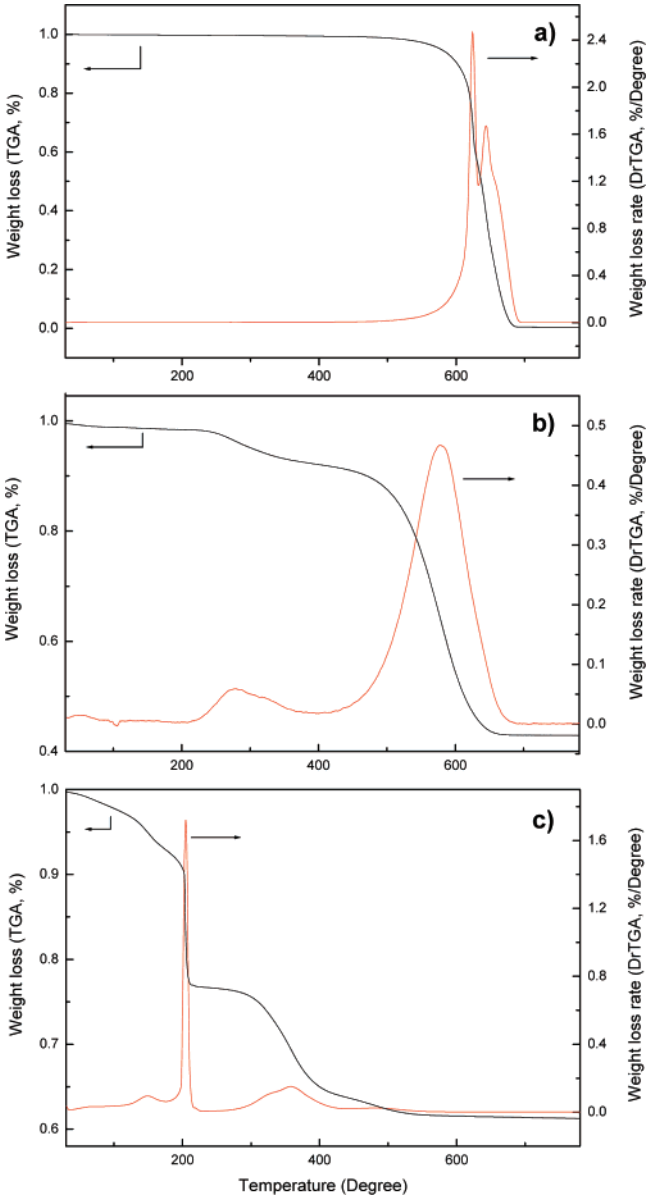

Figure 8. TGA and DrTGA curves of (a) as-received CNTs, (b) as-prepared TiO_2/CNTs nanocomposite, and (c) as-prepared Co_3O_4/CNTs nanocomposite.

and 533.8−533.4 eV in the three samples can be assigned to very similar surface oxygen species, although their chemical environments are varied.[50−52]

Due to the similarity between the two capping compounds (the OA and alkylated oleate groups) used, the surface information of C 1s and O 1s for the Co_3O_4 nanocubes is essentially similar to that reported in Figure 9, except they do not exhibit pronounced BE shifts. Detailed surface analyses for the dried Co_3O_4 nanocubes, the Co_3O_4/CNTs, and the sonicated Co_3O_4/CNTs nanocomposites can be found in the Supporting Information (SI-9). Therefore, it can be deduced that the electronic interaction between the Co_3O_4 nanocubes and CNTs substrate is not strong in this binary system.

As a final note of this report, to test the applicability of the above self-assembled nanocomposites in real working environ-

(48) Ebbesen, T. W.; Hiura, H.; Bisher, M. E.; Treacy, M. M. J.; Shreeve-Keyer, J. L.; Haushalter, R. C. *Adv. Mater.* **1996**, *8*, 155−157.
(49) Yu, R.; Chen, L.; Liu, Q.; Lin, J.; Tan, K. L.; Ng, S. C.; Chan, H. S. O.; Xu, G. Q.; Hor, T. S. A. *Chem. Mater.* **1998**, *10*, 718−722.
(50) Hiura, H.; Ebbesen, T. W.; Tanigaki, K. *Adv. Mater.* **1995**, *7*, 275−276.
(51) Kwon, J. Y.; Kim, H. D. *J. Appl. Polym. Sci.* **2005**, *96*, 595−604.
(52) Chen, L.; Zhang, B. L.; Qu, M. Z.; Yu, Z. L. *Powder Technol.* **2005**, *154*, 70−72.

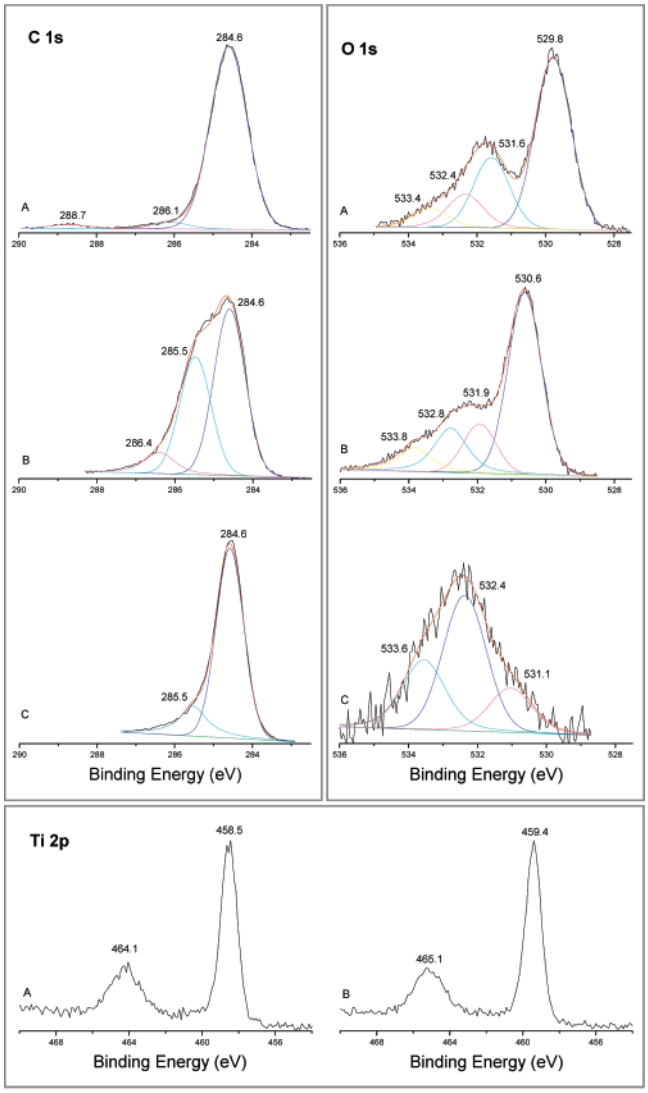

Figure 9. XPS spectra of C 1s, O 1s, and Ti 2p: (A) dried TiO_2 powder, (B) the TiO_2/CNTs nanocomposite, and (C) as-received CNTs.

ments, we selected the TiO_2/CNTs system as a model case for Li-battery application.[53−71] Our electrochemical testing results show that the reversible capacity of this cathode material can maintain at about 225 mA h g^{-1}, which is about 17% higher than a reported capacity of hydrogen titanate nanowires (191.8 mA h g^{-1}),[69] about 32% higher than that of nanosized rutile TiO_2 (∼170 mA h g^{-1}),[62] and about 50% higher than that of anatase TiO_2 (∼150 mA h g^{-1}).[60] Details on the experimental procedure and related discussion of this application study can be obtained from the Supporting Information (SI-11).

Conclusions

In summary, we have devised a step-by-step self-assembly approach for preparation of binary, ternary and quaternary CNTs-based nanocomposites using presynthesized nanoparticles as primary building units. In particular, six material combinations, TiO_2/CNTs, Co_3O_4/CNTs, Au/CNTs, Au/TiO_2/CNTs, TiO_2/Co_3O_4/CNTs, and Co/CoO/Co_3O_4/CNTs, have been prepared under either sonication or simple mechanical stirring condition. Through materials characterization and a series of designed experiments, interactions and interconnectivity between the overlayers and CNTs can be better understood. We have demonstrated that good controls in particle shape, size, and distribution for these highly complex inorganic−organic nanocomposites and nanohybrids can be further attained. For example, the content of overlayer components can be easily controlled by predetermining ratios of assembled components (i.e., overlayer/CNTs ratios) and assembling time. In general, a greater ratio of overlayer/CNTs and a longer processing time will lead to a higher loading of the surface phase(s). Concerning their actual applications, furthermore, we have illustrated that self-assembled TiO_2/CNTs is sufficiently robust and the electrochemical performance of TiO_2 phase is significantly enhanced when the composite is used as a potential cathode material in Li-battery application. In view of its process simplicity (e.g., room-temperature assembling process, etc.), the present self-assembly approach shows a good potential for large-scale synthesis. In principle, even more complex nanocomposites, including quaternary and other higher ordered derivatives, of metals and metal oxides with CNTs should also be attainable using the general findings reported in this work.

Acknowledgment. The authors gratefully acknowledge the financial support of the Ministry of Education, Singapore.

Supporting Information Available: XRD, TEM, EDX, XPS, and data from electrochemical investigation. This material is available free of charge via the Internet at http://pubs.acs.org.

JA071122V

(53) Bavykin, D. V.; Friedrich, J. M.; Walsh, F. C. *Adv. Mater.* **2006**, *18*, 2807−2824.
(54) Stura, E.; Nicolini, C. *Anal. Chim. Acta* **2006**, *568*, 57−64.
(55) Exnar, I.; Kavan, L.; Huang, S. Y.; Grätzel, M. *J. Power Sources* **1997**, *68*, 720−722.
(56) Gao, X.; Zhu, H.; Pan, G.; Ye, S.; Lan, Y.; Wu, F.; Song, D. *J. Phys. Chem. B* **2004**, *108*, 2868−2872.
(57) Moriguchi, I.; Hidaka, R.; Yamada, H.; Kudo, T.; Murakami, H.; Nakashima, N. *Adv. Mater.* **2006**, *18*, 69−73.
(58) Kavan, L.; Rathouský, J.; Grätzel, M.; Shklover, V.; Zukal, A. *J. Phys. Chem. B* **2000**, *104*, 12012−12020.
(59) Kavan, L.; Kalbáč, M.; Zukalová, M.; Exnar, I.; Lorenzen, V.; Nesper, R.; Grätzel, M. *Chem. Mater.* **2004**, *16*, 477−485.
(60) Sudant, G.; Baudrin, E.; Larcher, D.; Tarascon, J. M. *J. Mater. Chem.* **2005**, *15*, 1263−1269.
(61) Lindström, H.; Södergren, S.; Solbrand, A.; Rensmo, H.; Hjelm, J.; Hagfeldt, A.; Lindquist, S. E. *J. Phys. Chem. B* **1997**, *101*, 7717−7722.
(62) Hu, Y. S.; Kienle, L.; Guo, Y. G.; Maier, J. *Adv. Mater.* **2006**, *18*, 1421−1426.
(63) Armstrong, A. R.; Armstrong, G.; Canales, J.; Bruce, P. G. *Angew. Chem., Int. Ed.* **2004**, *43*, 2286−2288.
(64) Armstrong, A. R.; Armstrong, G.; Canales, J.; Garcia, R.; Bruce, P. G. *Adv. Mater.* **2005**, *17*, 862−865.
(65) Wang, Y.; Lee, J. Y.; Zeng, H. C. *Chem. Mater.* **2005**, *17*, 3899−3903.
(66) Kim, Y. A.; Kojima, M.; Muramatsu, H.; Umemoto, S.; Watanabe, T.; Yoshida, K.; Sato, K.; Ikeda, T.; Hayashi, T.; Endo, M.; Terrones, M.; Dresselhaus, M. S. *Small* **2006**, *2*, 667−676.
(67) Shin, H. C.; Liu, M.; Sadanadan, B.; Rao, A. M. *J. Solid State Electrochem.* **2004**, *8*, 908−913.
(68) Tang, S. B.; Xia, H.; Lai, M. O.; Lu, L. *J. Electrochem. Soc.* **2006**, *153*, A875−A879.
(69) Li, J.; Tang, Z.; Zhang, Z. *Chem. Mater.* **2005**, *17*, 5848−5855.
(70) Kavan, L.; Attia, A.; Lenzmann, F.; Elder, S. H.; Grätzel, M. *J. Electrochem. Soc.* **2000**, *147*, 2897−2902.
(71) van der Krol, R.; Goossens, A.; Meulenkamp, E. A. *J. Electrochem. Soc.* **1999**, *146*, 3150−3154.